14

Double "Fermi" Phase Shift Functions

We shall here consider the superposition of two "Fermi" functions having different ranges, $c \neq c'$, and different surface thicknesses, $\beta \neq \beta'$. Thus, the two phase shift functions that we combine have the same functional form, and their derivatives have singularities of the same degree. Asymptotically, they will thus "attract" the points of stationary phase with equal strength, but the numerical values of the various parameters will determine which singularities are more relevant.

If we denote the basic "Fermi" distribution

$$X_{\mathrm{F}}(c,\beta,b_x) = \frac{A_{\mathrm{F}}}{1+\exp[(b_x-c)/\beta]}, \tag{14.1}$$

then one could imagine combining such functions either in a multiplicative way

$$[X_{\mathrm{F}}(c,\beta,b_x)+1]\,X_{\mathrm{F}}(c',\beta',b_x), \tag{14.2}$$

or, in an additive way, as

$$X_{\mathrm{F}}(c,\beta,b_x) + X_{\mathrm{F}}(c',\beta',b_x). \tag{14.3}$$

We shall in this chapter explore this second option:

$$X(b_x) = \frac{A_{\mathrm{F}}}{1+\exp[(b_x-c)/\beta]} + \frac{A'_{\mathrm{F}}}{1+\exp[(b_x-c')/\beta']}, \quad \mathrm{Re}\, b_x > 0, \tag{14.4}$$

with A_{F} and A'_{F} complex and $X(-b_x) = X(b_x)$. In the context of absorption, various cases come to mind: the second function can be exploited to provide more (or less) absorption in the inner region,

$$|A_{\mathrm{F}} + A'_{\mathrm{F}}| > |A_{\mathrm{F}}| \quad \text{or} \quad |A_{\mathrm{F}} + A'_{\mathrm{F}}| < |A_{\mathrm{F}}|, \quad c' < c. \tag{14.5}$$

Another possibility would be to let the real and absorptive parts have different ranges.

Downloaded from https://www.cambridge.org/core. UNIVERSIDAD AUTONOMA METROPOLITANA, on 10 Nov 2026 at 21:30:45, subject to the Cambridge Core terms of use, available at https://www.cambridge.org/core/terms. https://doi.org/10.1017/9781316219256.018

Even within this family of functions Eq. (14.4), there are many ways of choosing $A'_{\rm F}$, c', and β' relative to $A_{\rm F}$, c, and β. We first explore the case $\beta = \beta'$, and in a second section let β be different from β'.

14.1 Two "Fermi" Phase Shift Functions with the Same Surface Thickness

14.1.1 Additional Internal Structure

We start out by studying the two cases

$$X_p(b_x) = \frac{A_{\rm F}}{1+\exp[(b_x-c)/\beta]} + \frac{A'_{\rm F}}{1+\exp[(b_x-c')/\beta]}, \quad \mathrm{Re}\, b_x > 0, \quad (14.6a)$$

$$X_m(b_x) = \frac{A_{\rm F}}{1+\exp[(b_x-c)/\beta]} - \frac{A'_{\rm F}}{1+\exp[(b_x-c')/\beta]}, \quad \mathrm{Re}\, b_x > 0, \quad (14.6b)$$

for purely imaginary phase shift functions with parameters

$$A_{\rm F} = i, \quad c = 3 \text{ fm}, \quad A'_{\rm F} = 0.2i, \quad c' = 2 \text{ fm}, \quad \beta = 0.5 \text{ fm}. \quad (14.7)$$

These phase shift functions are presented in Fig. 14.1 for $A'_{\rm F} = 0.2i$ (dashed) with $A'_{\rm F} = 0$ (solid) as a reference.

In order to get an overview over possible locations of stationary points, we start out by showing in Figs. 14.2 and 14.3 the corresponding "maps" of possible stationary points. These are along lines where $X'(b_x)$ is real ($\mathrm{Im}\, X'(b_x) = 0$, dashed), and where $\mathrm{Re}\, X'(b_x) > 0$ (white regions). As for the "Fermi" phase shift function discussed in Chapter 8, there are trajectories of stationary points in the regions

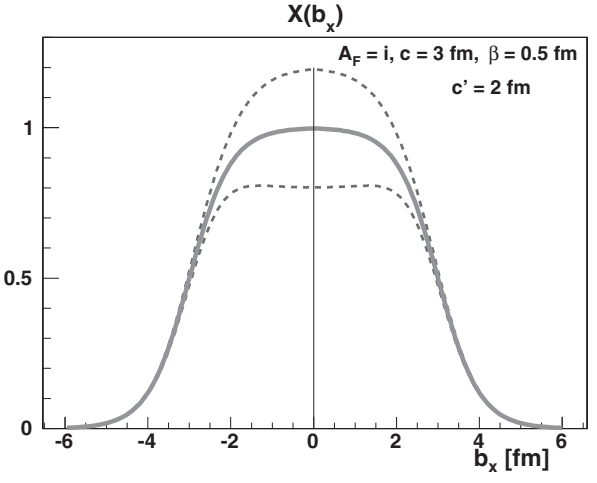


Figure 14.1 Dashed: sum and difference of two "Fermi" phase shift functions having different ranges, but the same surface thickness. Solid: Single "Fermi" phase shift function (reference).

Downloaded from https://www.cambridge.org/core. UNIVERSIDAD AUTONOMA METROPOLITANA, on 10 Nov 2026 at 21:30:45, subject to the Cambridge Core terms of use , available at https://www.cambridge.org/core/terms. https://doi.org/10.1017/9781316219256.018

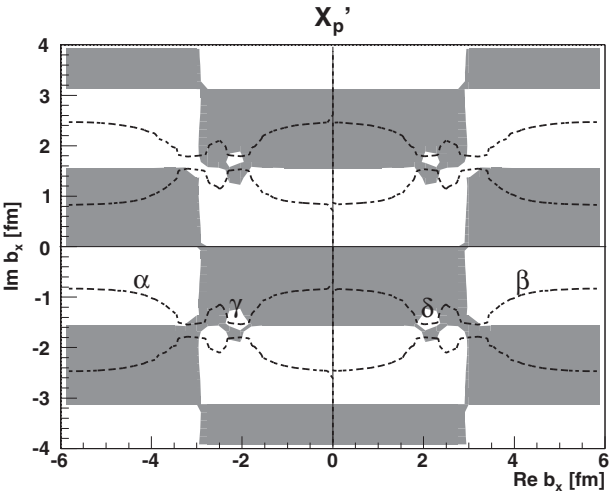


Figure 14.2 Regions of positive and negative values of $\mathrm{Re}\, X'(b_x)$, shown in the complex b_x-plane for the sum of two "Fermi" phase shift functions Eq. (14.6a), with the parameters of Eq. (14.7).

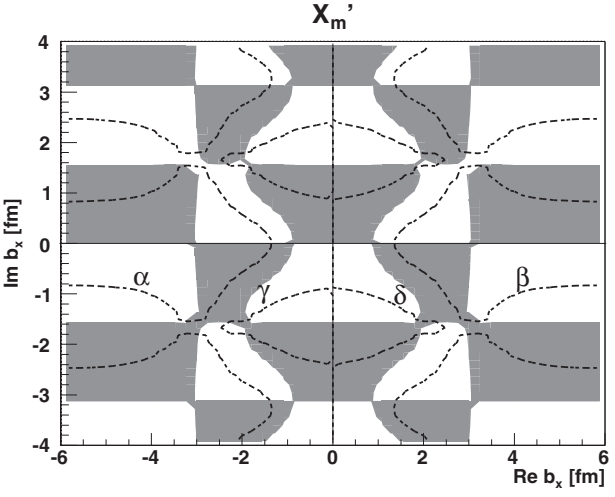


Figure 14.3 Regions of positive and negative values of $\mathrm{Re}\, X'(b_x)$, shown in the complex b_x-plane for the difference of two "Fermi" phase shift functions Eq. (14.6b), with the parameters of Eq. (14.7).

(white rectangles) $|\mathrm{Re}\, b_x| > c$, $-\pi\beta/2 < \mathrm{Im}\, b_x < 0$. These provide the dominant contributions to the cross sections, and are labeled α and β. Asymptotically, as $q \to \infty$, they approach the pole singularities, $\mp c - i\pi\beta$. In addition, due to the structure provided by the second "Fermi" distribution, there are stationary points γ and δ near $\mp c' - i\pi\beta$.

Downloaded from https://www.cambridge.org/core. UNIVERSIDAD AUTONOMA METROPOLITANA, on 10 Nov 2026 at 21:30:45, subject to the Cambridge Core terms of use , available at https://www.cambridge.org/core/terms. https://doi.org/10.1017/9781316219256.018

We recall that we seek a deformation of the contour of integration, from $b_x = -\infty$ to $b_x = +\infty$, down into the complex plane ($\mathrm{Im}\, b_x < 0$) such that the integral can be associated with the contributions from a few points of stationary phase, or saddle points. For large values of the momentum transfer q, these will be in the neighborhoods of the singularities of $X'(b_x)$.

Let us consider the situation in the fourth quadrant, where the composite phase shift function $X(b_x)$ has simple poles at $b_x = c - i\pi\beta$ and $b_x = c' - i\pi\beta$. The derivative, $X'(b_x)$ will have double poles at these locations. If we expand b_x around one such point as $b_x - b_x^{\mathrm{pole}} = \rho^{i\theta}$, the derivative will for A_{F} imaginary behave as $X' \sim (i/\rho^2)e^{-2i\theta}$. In order to match the (real) momentum transfer, this quantity has to be real at the stationary point,

$$\mathrm{Im}\left(ie^{-2i\theta}\right) = 0, \quad \text{or} \quad \theta = \frac{\pi}{4} + \frac{n\pi}{2}. \tag{14.8}$$

Among these four directions, indicated by dashed curves in Figs. 14.2 and 14.3, X' is positive at every other, namely at $\theta = \pi/4$ and $\theta = 5\pi/4$. But, as for the single "Fermi" function studied in Section 8.4, the path of integration passes through only one of them (here denoted β). In the language of saddle points, the other is behind the "ridge" and will not be encountered along the path of integration. Likewise, γ and δ are on the side of the corresponding poles that is closer to the real axis.

For the case Eq. (14.6b), there will be a different approach to the singularities at $\mp c' - i\pi\beta$ due to the overall minus sign associated with this "secondary" "Fermi" function. In the language of Eq. (14.8), in the fourth quadrant the relevant X' is positive at $\theta = -\pi/4$ and $\theta = 3\pi/4$. Again, the points γ and δ are on the side of the corresponding poles that is closer to the real axis.

Fig. 14.4 is devoted to the differential cross sections produced by the phase shift function X_p of Eq. (14.6). It is shown together with the corresponding one for only one "Fermi" phase shift function, $A'_{\mathrm{F}} = 0$. There is an almost complete overlap. Actually, the X_m case is also similar. In this particular case of X_p, we have checked that a numerical evaluation of the diffraction integral agrees well with the asymptotic result for the differential cross section from the maximum around 10^4 mb/(GeV/c) at small momentum transfers down to a magnitude level of around 10^{-17} mb/(GeV/c).

The agreement between the cross sections with $A'_{\mathrm{F}} = \pm 0.2i$ and $A'_{\mathrm{F}} = 0$ is partly due to the smallness of the contributions from the additional points of stationary phase, γ and δ, and perhaps even more to the very slow movement of the stationary points along the dominant trajectories α and β. The trajectories are shown in the inset in Fig. 14.4, and in Fig. 14.5 we show β and δ (whose real parts are positive) in more detail. The dominant trajectory (in the fourth quadrant) is practically the same for these three cases, both for the real part and for the imaginary part. For the δ

Downloaded from https://www.cambridge.org/core. UNIVERSIDAD AUTONOMA METROPOLITANA, on 10 Nov 2026 at 21:30:45, subject to the Cambridge Core terms of use, available at https://www.cambridge.org/core/terms. https://doi.org/10.1017/9781316219256.018

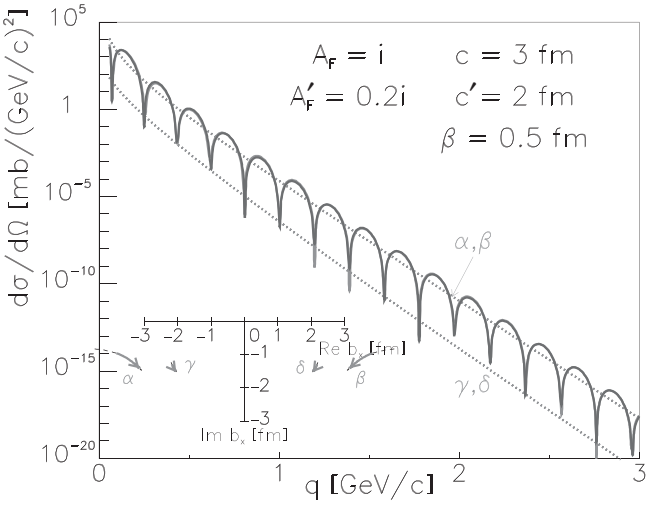


Figure 14.4 Differential cross sections corresponding to the phase shift function Eq. (14.6). The cases of $A_F = 0.2i$ and $A_F = 0$ are completely overlapping. The inserts show the trajectories of stationary points for $0.02\ \mathrm{GeV/c} \leq q \leq 5.0\ \mathrm{GeV/c}$ (dotted). The cross sections contributed by the individual stationary points are shown as dotted curves, labeled α, β and γ, δ.

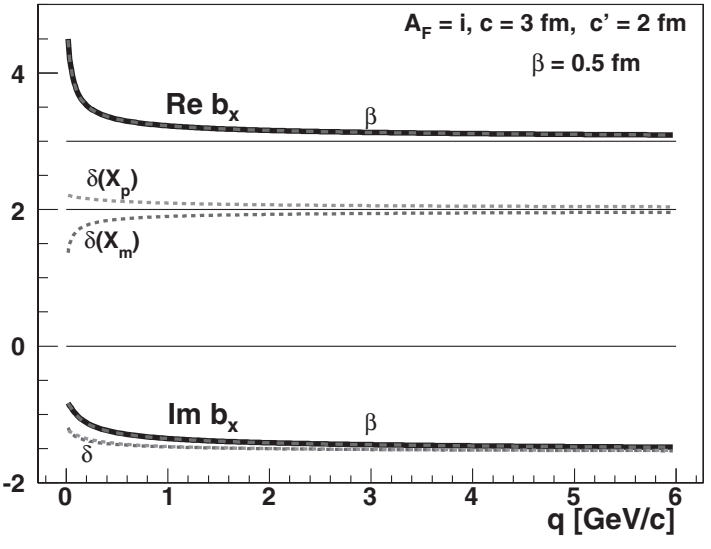


Figure 14.5 Real and imaginary parts of b_x at stationary points β and δ, for a range of momentum transfer q.

Downloaded from https://www.cambridge.org/core. UNIVERSIDAD AUTONOMA METROPOLITANA, on 10 Nov 2026 at 21:30:45, subject to the Cambridge Core terms of use, available at https://www.cambridge.org/core/terms. https://doi.org/10.1017/9781316219256.018

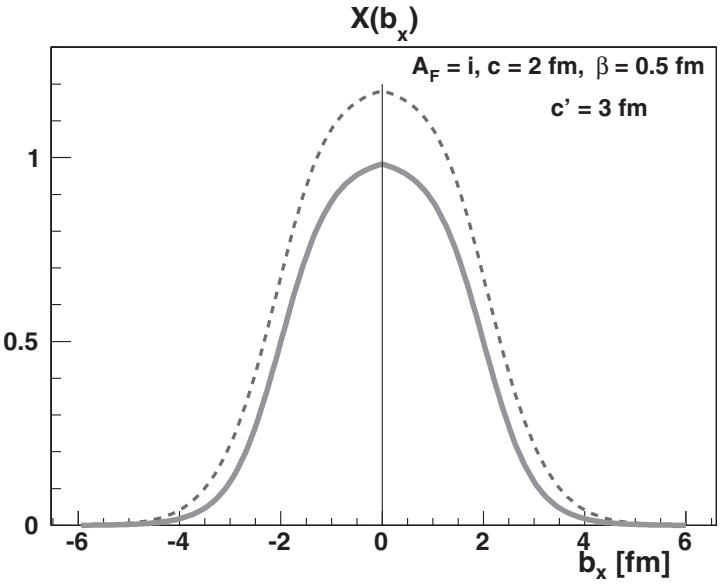


Figure 14.6 "Fermi" phase shift functions. Solid: Single reference function ($A'_{\rm F} = 0$). Dashed: sum of two "Fermi" phase shift functions having different ranges, but the same surface thickness, with parameters given by Eq. (14.9).

trajectory, there is in the real part, at small momentum transfers, a small difference between the two cases of X_p and X_m, whereas the imaginary parts are essentially the same.

14.1.2 Additional External Structure

What happens if the outer distribution is subdominant, in the sense that $|A'_{\rm F}| < |A_{\rm F}|$ with $c' > c$? We display in Fig. 14.6 the phase shift function for such a case, with

$$A_{\rm F} = i, \quad c = 2 \text{ fm}, \quad A'_{\rm F} = 0.2i, \quad c' = 3 \text{ fm}, \quad \beta = 0.5 \text{ fm}, \tag{14.9}$$

compared with the case of $A'_{\rm F} = 0$. The two phase shift functions look qualitatively rather similar, but the double one has an extra pair of stationary points, which for this case are most important.

In Fig. 14.7 we show the "map" of possible stationary points, for the composite phase shift function defined by the parameters of Eq. (14.9). The outer ones, asymptotically approaching the singularities at $b_x = \mp c' - i\pi\beta$ are labeled α and β, whereas the inner ones near $b_x = \mp c - i\pi\beta$ are labeled γ and δ. The corresponding single phase shift function, for $A'_{\rm F} = 0$, will have the trajectories α and β connected to the regions of γ and δ.

Downloaded from https://www.cambridge.org/core. UNIVERSIDAD AUTONOMA METROPOLITANA, on 10 Nov 2026 at 21:30:45, subject to the Cambridge Core terms of use, available at https://www.cambridge.org/core/terms. https://doi.org/10.1017/9781316219256.018

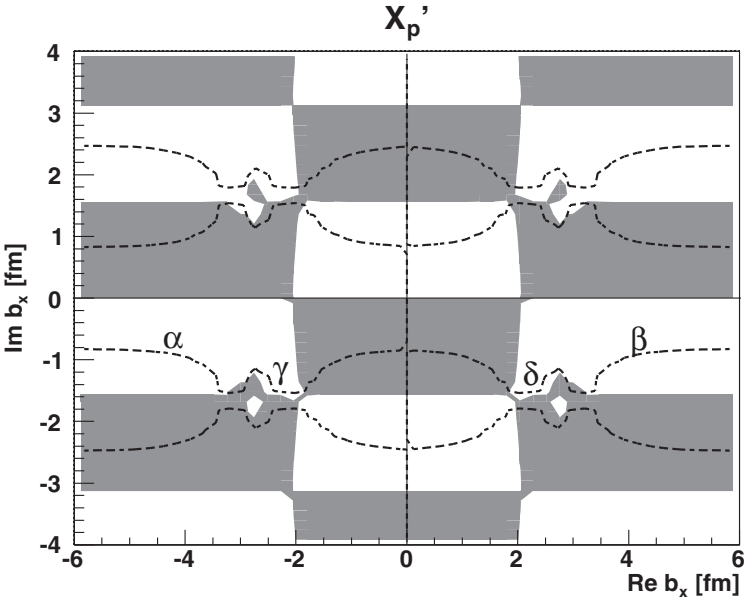


Figure 14.7 Regions of positive and negative values of $\mathrm{Re}\, X'(b_x)$, shown in the complex b_x-plane for the sum of two "Fermi" phase shift functions Eq. (14.6a), with the parameters of Eq. (14.9).

At small momentum transfers, the outer stationary points (α and β) will provide the dominant contributions, since they are closer to the real axis. However, as the momentum transfer increases, these will gradually be forced further down into the complex plane, "attracted" by the external singularities at $\mp c - i\pi\beta$. Then, in some range of momentum transfer, where the two pairs of stationary points (α, β) and (γ, δ) are at similar distances from the real axis, they will provide comparable contributions to the overall scattering amplitude. However, the pair (γ, δ) is closer to each other than the pair (α, β), and therefore leads to oscillations of a longer period.

In Fig. 14.8 we show the resulting differential cross section (solid), and compare with the case of $A'_{\mathrm{F}} = 0$ (dashed). While the single "Fermi" phase shift function provides a rather periodic diffraction pattern, the composite one yields at intermediate momentum transfers a more "irregular" pattern. At small momentum transfers it provides a somewhat shorter period of oscillations, corresponding to the contributions of the outer stationary points (α, β) which there (at small momentum transfers) are important. Eventually, as the momentum transfer increases, these contributions are no longer dominant, and those from the inner points of stationary phase, (γ, δ) take over, yielding a longer period of oscillation.

Downloaded from https://www.cambridge.org/core. UNIVERSIDAD AUTONOMA METROPOLITANA, on 10 Nov 2026 at 21:30:45, subject to the Cambridge Core terms of use, available at https://www.cambridge.org/core/terms. https://doi.org/10.1017/9781316219256.018

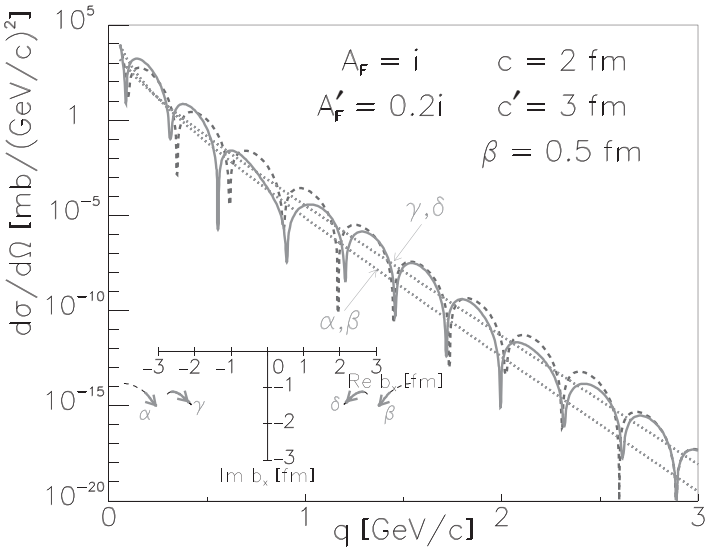


Figure 14.8 Differential cross sections corresponding to the phase shift function Eq. (14.6). The cases of $A'_F = 0.2i$ (solid) and $A'_F = 0$ (dashed) are compared. The inserts show the trajectories of stationary points for $0.02\ \text{GeV/c} \le q \le 5.0\ \text{GeV/c}$ (dotted). The cross sections contributed by the individual stationary points are shown as dotted curves, labeled α, β and γ, δ.

Thus, while the differential cross section shown in Fig. 14.4 displays 15 maxima over the range of momentum transfers out to $q = 3$ GeV/c, Fig. 14.8 displays only 10. It is of course no accident that this ratio is that of c'/c.

14.2 Different Surface Thicknesses

The picture can change qualitatively if the two phase shift functions have rather different surface thicknesses. We shall discuss in turn the two cases of an additional external sharper structure, and an internal one, as compared to the "main" phase shift function, with $|A_F| = 1$.

14.2.1 Sharper External Structure

As a first case, let us consider an additional external structure ($c' > c$) which is sharper ($\beta' < \beta$) than the dominant one ($|A_F| = 5|A'_F|$):

$$\begin{aligned} A_F &= i \qquad c = 3\ \text{fm} \qquad \beta = 0.50\ \text{fm} \\ A'_F &= 0.2i \quad c' = 3.1\ \text{fm} \quad \beta' = 0.25\ \text{fm} \end{aligned} \tag{14.10}$$

The corresponding "map" of possible stationary points is shown in Fig. 14.9. The main part of the phase shift function provides the trajectories of stationary

Downloaded from https://www.cambridge.org/core. UNIVERSIDAD AUTONOMA METROPOLITANA, on 10 Nov 2026 at 21:30:45, subject to the Cambridge Core terms of use, available at https://www.cambridge.org/core/terms. https://doi.org/10.1017/9781316219256.018

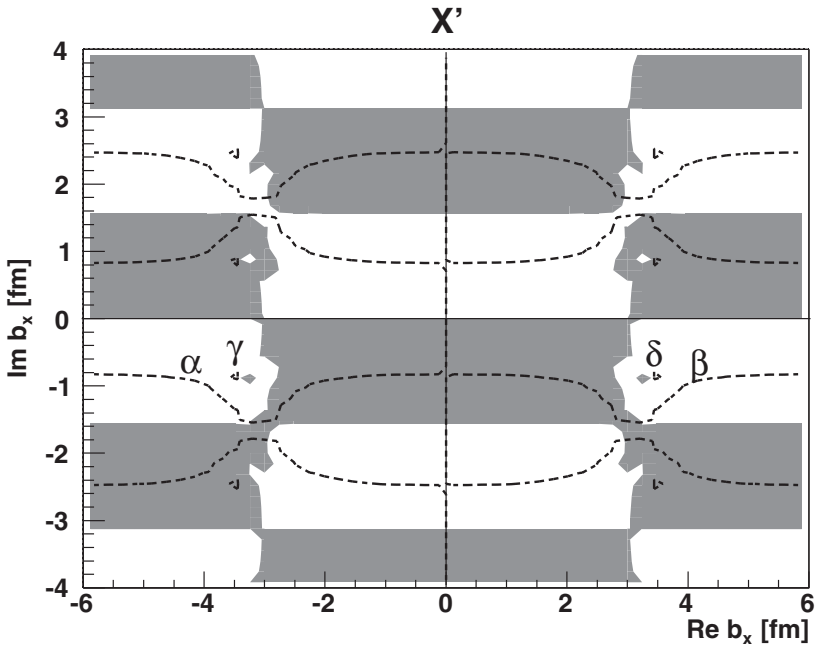


Figure 14.9 Regions of positive and negative values of $\mathrm{Re}\, X'(b_x)$, shown in the complex b_x-plane for the sum of two "Fermi" phase shift functions Eq. (14.6a), with the parameters of Eq. (14.10).

points labeled α and β, coming in from $\mathrm{Re}\, b_x = \pm\infty$, below the real axis. The sharp outer edge provides additional stationary points, labeled γ and δ in this figure. They are confined to a very small region (indicating little dependence on the momentum transfer) and are of course closer to the real axis, since the corresponding β' is smaller.

It is interesting that the trajectories extending out to $\mathrm{Re}\, b_x \to \pm\infty$, are *not* those associated with the outer structure, at $c' = 3.1$ fm $> c$, but instead those associated with the softer edge, $\beta > \beta'$. However, as $|A'_{\mathrm{F}}|$ increases, the trajectories associated with the singularities at $\mp c' - i\pi\beta'$ will become more important. Indeed, for $|A'_{\mathrm{F}}|$ of the order of 0.4 or larger (and the other parameters as defined by Eq. (14.10)), the trajectories coming in from $\mp\infty$ will end at the outermost singularities, $\mp c' - i\pi\beta'$. Then, there will, on the other hand, be trajectories of finite extensions associated with the singularities at $\mp c - i\pi\beta$.

For sufficiently large momentum transfers, when the trajectories α and β move further away from the real axis, the contributions of γ and δ will take over and dominate. This is seen in the differential cross section plot, Fig. 14.10, where we also show the reference cross section (dashed) for $A'_{\mathrm{F}} = 0$. The reference cross section is determined by the stationary points α and β, which are practically unchanged, in analogy with the case shown in Fig. 14.5.

Downloaded from https://www.cambridge.org/core. UNIVERSIDAD AUTONOMA METROPOLITANA, on 10 Nov 2026 at 21:30:45, subject to the Cambridge Core terms of use, available at https://www.cambridge.org/core/terms. https://doi.org/10.1017/9781316219256.018

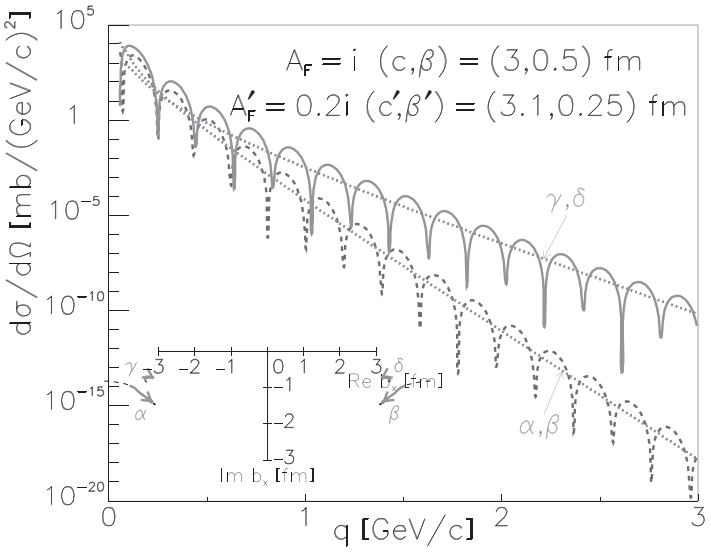


Figure 14.10 Differential cross sections corresponding to the phase shift function Eq. (14.10). The cases of $A'_F = 0.2i$ (solid) and $A'_F = 0$ (dashed) are compared. The inserts show the trajectories of stationary points for $0.02\ \text{GeV/c} \le q \le 5.0\ \text{GeV/c}$ (dotted). The cross sections contributed by the individual stationary points are shown as dotted curves, labeled α, β and γ, δ.

Clearly, for a smaller outer structure (a smaller value of $|A'_F|$), this "take-over" would be postponed to higher momentum transfers.

14.2.2 Sharper Internal Structure

As an example of additional, sharper internal structure, we consider the case

$$\begin{aligned} A_F &= i \qquad c = 3.0\ \text{fm} \quad \beta = 0.50\ \text{fm} \\ A'_F &= 0.2i \quad c' = 2.9\ \text{fm} \quad \beta' = 0.40\ \text{fm} \end{aligned} \tag{14.11}$$

The relevant "map" of possible stationary points is shown in Fig. 14.11. As in the previous case, there are trajectories of stationary points (denoted α and β) coming in from $\text{Re}\, b_x = \mp\infty$ towards the singularities at $\mp c - i\pi\beta$, and additional stationary points γ and δ associated with the singularities at $\mp c' - i\pi\beta'$, again of finite extension.

When there are two nearby singularities, the angle of approach may deviate significantly from the more typical $\pm 45^\circ$ discussed in Chapter 8 and Eq. (14.8), since the "landscape" defined by the magnitude of the diffraction integrand

$$\exp[q\ \text{Im}\, b_x - \ \text{Im}\, X(b_x)] \tag{14.12}$$

can get very distorted.

Downloaded from https://www.cambridge.org/core. UNIVERSIDAD AUTONOMA METROPOLITANA, on 10 Nov 2026 at 21:30:45, subject to the Cambridge Core terms of use, available at https://www.cambridge.org/core/terms. https://doi.org/10.1017/9781316219256.018

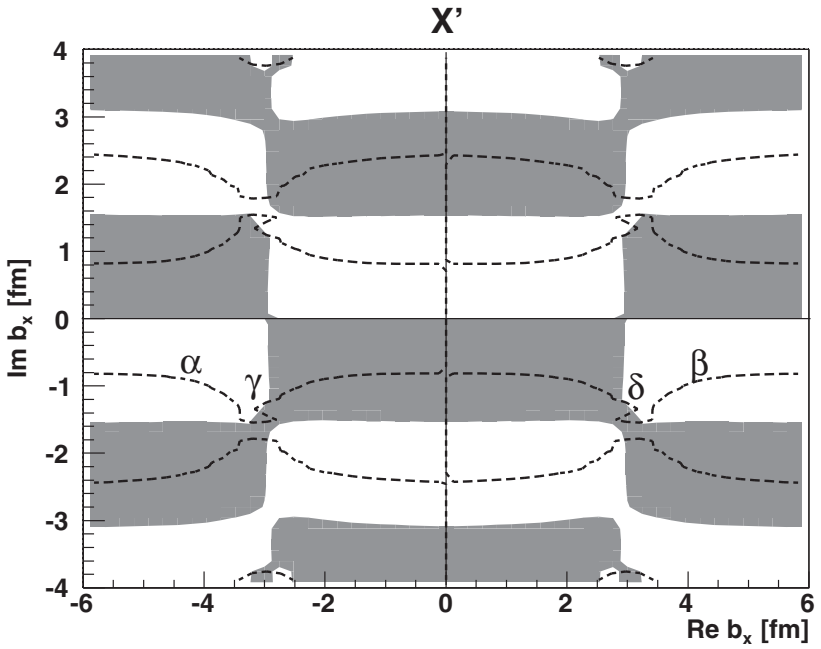


Figure 14.11 Regions of positive and negative values of $\mathrm{Re}\, X'(b_x)$, shown in the complex b_x-plane for the sum of two "Fermi" phase shift functions Eq. (14.6a), with the parameters of Eq. (14.11).

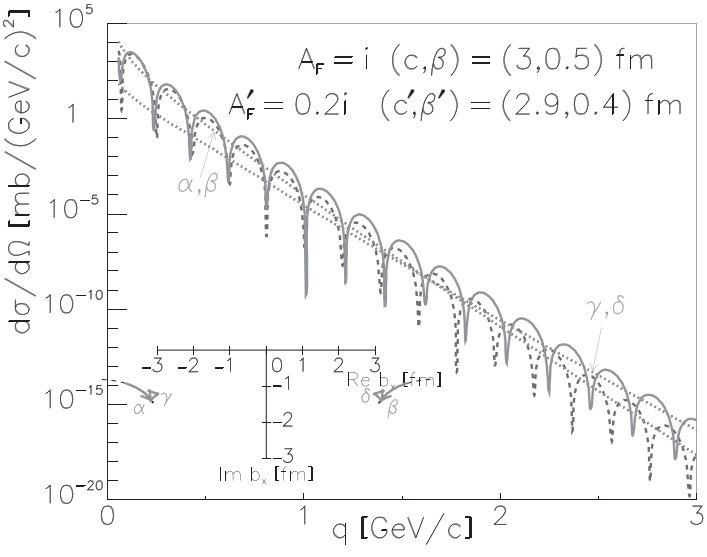


Figure 14.12 Differential cross sections corresponding to the phase shift function Eq. (14.11). The cases of $A'_{\mathrm{F}} = 0.2i$ (solid) and $A'_{\mathrm{F}} = 0$ (dashed) are compared. The inserts show the trajectories of stationary points for $0.02\ \mathrm{GeV/c} \leq q \leq 5.0\ \mathrm{GeV/c}$ (dotted). The cross sections contributed by the individual stationary points are shown as dotted curves, labeled α, β and γ, δ.

Downloaded from https://www.cambridge.org/core. UNIVERSIDAD AUTONOMA METROPOLITANA, on 10 Nov 2026 at 21:30:45, subject to the Cambridge Core terms of use, available at https://www.cambridge.org/core/terms. https://doi.org/10.1017/9781316219256.018

In Fig. 14.12 we show the corresponding differential cross section. It is seen that the contributions from α and β will dominate at small momentum transfers, whereas the contributions from γ and δ gradually take over at larger momentum transfers. Here, as the contributions from γ and δ start to dominate, the period of oscillation is seen to become longer, in agreement with their larger separation.

A common feature seen in many of the cases studied in this chapter is that when a "secondary" set of stationary points takes over at large momentum transfers, and perhaps provides a different period of oscillation, then this is associated with a less steep envelope of the differential cross section. The reason is that in order to become dominant, the additional structure must be sharper, meaning that the singularity must be closer to the real axis in the complex b_x-plane.

Downloaded from https://www.cambridge.org/core. UNIVERSIDAD AUTONOMA METROPOLITANA, on 10 Nov 2026 at 21:30:45, subject to the Cambridge Core terms of use , available at https://www.cambridge.org/core/terms. https://doi.org/10.1017/9781316219256.018